Proceedings of The National Conference
On Undergraduate Research (NCUR) 2019
Kennesaw State University
Kennesaw, Georgia
April 11-13, 2019

Homogeneous Sol-gel Coating of Manganese Dioxide Nanofibers to Prevent Cathode Dissolution

Zeljka Zec, Milan Haddad
Department of Chemistry and Biochemistry
370 Paulding Avenue NW
Kennesaw, GA 30144

Faculty Advisor: Altug S. Poyraz

Abstract

The cathode dissolution is a known phenomenon for manganese dioxide (MnO_2) based cathode materials in both aqueous and non-aqueous batteries. Upon battery discharge, reduced Mn^{3+} species disproportionate ($2Mn^{3+} \rightarrow Mn^{4+} + Mn^{2+}$) and Mn^{2+} dissolves into the electrolyte causing the loss of active material. While MnO_2 is a promising cathode for rechargeable aqueous zinc ion batteries (ZIB) due to its availability and low toxicity, the electrochemical performance is limited during battery cycling due to the dissolution of the cathode. In this work, a homogeneous sol-gel SiO_2 coatings with various thicknesses (0.5-5nm) on α-MnO_2 nanorods are reported. The sol-gel SiO_2 coating is achieved by hydrolysis-condensation of TEOS (tetraethyl orthosilicate) under mild reflux conditions. Further in-depth characterization of SiO_2 coated α-MnO_2 are done by XRD, Raman, FTIR, BET, XPS and SEM/TEM to analyze the surface of the silica coated α-MnO_2 cathodes. The electrochemical performance of the SiO_2 coated α-MnO_2 cathodes are studied in two electrode zinc batteries at room temperatures. The cathode dissolution is investigated by determining the Mn^{2+} content in the electrolyte and characterization of the used electrodes. This study will further benefit all different battery types that have the same cathode dissolution problem.

Keywords: Aqueous Zinc-ion batteries, Silica coating, Cathode dissolution

1. Introduction

Rechargeable aqueous Zinc-ion batteries (ZIBs) have emerged in recent years as a safe and sustainable large-scale energy storage option. Specifically, in comparison to lithium-ion batteries, ZIBs utilize cheaper, less toxic, and more abundant materials, and they are inherently safer due to their aqueous electrolytes with relatively nontoxic Zn^{2+} and Mn^{2+} ions. Recent research in aqueous Zinc-ion batteries explores the potential to prolong cycling life by utilizing different electrolytes, different tunnel and layer-structured cathode materials, reducing corrosion of the zinc anode and mitigating cathode dissolution[1,2,3].

Cryptomelane-type α-MnO_2 in particular is a promising cathode material with a large theoretical discharge capacity (300 mA/g) and good cyclability[4]. However, certain limitation of ZIBs utilizing α-MnO_2 include the formation of other manganese oxide phases during cycling, the questionable integrity of the crystal structure of the α-MnO_2, controversy over the reaction mechanism in aqueous ZIBs, and dissolution of the MnO_2 cathode material[5,6,7]. Cathode dissolution is directly responsible for decreased cycling performance and has been reported across a variety of battery types[7]. As the battery cycles, active material dissolves into the electrolyte causing severe capacity loss. Currently, efforts being made to mitigate cathode dissolution include use of Mn^{2+} electrolyte additive, Zinc surface doping of cathode and cathode surface modifications[8,9].

This study investigates the application of SiO_2 surface coating on α-MnO_2 nanorods and its effect on reducing the cathode dissolution. Cryptomelane-type α-MnO_2 nanorods were synthesized using a reflux method and subsequently

coated with various percentages (wt.%) of SiO_2. The silica-coated MnO_2 was characterized and batteries were made from the α-MnO_2 (non-silica coated parent material), 0.2% silica, and 10% silica-coated α-MnO_2 samples. Cyclic voltammetry and galvanostatic Charge/Discharge tests were carried out to study the effects of surface silica coating on battery performance, and used electrodes were characterized to study the morphology of the cathode material after cycling. Cathode dissolution is also investigated using EDX to measure the total amount of Manganese deposited in the battery case and normalizing the values using an internal cobalt standard.

2. Experimental

2.1 Materials

Manganese Sulfate monohydrate ($MnSO_4•H_2O$), > 99.0%), Potassium permanganate ($KMnO_4$, >99.0%), stainless steel gauze (325 mesh, type 316), carbon black (Super P > 99%), and Polytetrafluoroethylene (PTFE) were purchased from Alfa Aesar. Zinc Sulfate heptahydrate ($ZnSO_4•7H_2O$, 99.5%), Cobalt Acetate tetrahydrate ($Co(CH_3CO_2)_2•4H_2O$, 99%) and polymer Tetraethyl orthosilicate (TEOs, 98%) were purchased from Acros Organics. Ammonium Hydroxide solution (NH_4OH, 28.0-30.0%) was obtained from Beantown Chemical.

2.2 Materials Synthesis

Cryptomelane-type α-MnO_2 nanorods were synthesized under mild reflux conditions. Solution A contained 27.5 mmol (4.65 g) of Manganese Sulfate Monohydrate ($MnSO_4•H_2O$) with 20 mL of DI water while Solution B contained 18.5 mmol (2.92 g) of $KMnO_4$ (Potassium Permanganate) and 60 mL of DI water. Each one was placed in 100 mL round bottom flask and vigorously stirred until homogeneously dissolved. At room temperature, Solution A was slowly added to Solution B. dropwise. The mild reflux was done at 120°C for 24 hours. After filtration, the dark brownish-black precipitate was left in vacuum oven overnight to dry at 80ºC.

2.3 Silica Gel Coating

Silica gel coating was done experimentally to suppress cathode dissolution caused by zinc-ion battery discharging. TEOS, ethanol, water and Ammonium Hydroxide followed ratio of 1:100:400:20 respectively. In 50.0 mL round bottom flask, 0.25 g of α-MnO_2 (parent material) was added along with 20.0 mL ethanol, 23.0 mL of DI water, and 2.6 mL Ammonium Hydroxide with vigorous stirring in room temperature. Various concentrations (0.5 - 5 nm) of TEOS was prepared in a small vial along with 4.0 mL ethanol and mixed in with original solution. Stirring occurred for 12-16 h. Following, temperature controlled oil bath was employed and stirring was continued for 2-3 h at 70°C. After cooling, solution was filtered and placed in vacuum oven overnight for drying at 80ºC.

2.4 Materials Characterization

N_2-sorption (adsorption-desorption) isotherms were collected using Micromeritics ASAP 2020 Plus Instrument. The powder X-ray diffraction α -MnO_2 sample was degassed at 120° C for 6 h prior to the analyses. The surface areas were calculated using Brunaur-Emmett-Teller (BET) method. X-ray Diffraction (XRD) patterns were conducted using a Rigaku Miniflex XRD instrument (Cu Ka radiation l ¼ 1.5406 Å, 40 kV, and 20 mA) equipped with D/teX Ultra detector and monochromator. The measurements included 2θ =5- 70° range and with a step size of 0.02°. Scanning Electron Microscopy (SEM) images were taken using Tescan Vega at 30.0 kV to further analyze homogenous silica coating surroundings and MnO_2 fibers in different magnifications. Transmission Electron Microscopy (TEM) images of α-MnO_2 were recorded on a Hitachi HT-7700 TEM at 100 kV. X-ray photoelectron spectra (XPS) of used zinc electrodes were recorded on a Thermo K-alpha XPS (Al Ka radiation, l ¼ 1486.6 eV) instrument. The XPS spectra were analyzed using CASA-XPS software (Version 2.3). Further, Electron Dispersive Spectroscopy (EDS) atomic percentages were collected using Pathfinder software.

2.5 Electrochemical Characterization

Electrodes were made from α-MnO_2, 0.2%, and 10% silica-coated α-MnO_2 powders. Electrode paste was made by mixing cathode material (60% wt.), super-p conductive carbon (30% wt.), PTFE binder (10% wt.), and approximately 0.5 mL ethanol in a vial. The mixture was stirred until homogenous and left to dry into a paste. The electrode paste was then pressed onto stainless steel gauze circles and dried in an oven for 4-5 hours at 100ºC. Finally, the electrodes were pressed with a hydraulic press for 1 min. Batteries were made from the electrodes using filter paper separators, Zinc metal anodes, and 1.0 M $ZnSO_4$ electrolyte. Cyclic Charge/Discharge and Galvanostatic Cycling tests were conducted using a Gamry Interface 1010B Potentiostat/Galvanostat.

2.6 Dissolution Experiment

A control experiment was first conducted. Three 50 mL stock solutions of 10 mM $MnSO_4$, 10 mM $ZnSO_4$, and 4 mM $Co(CH_3COO)_2$ were prepared. 10 vials containing 2.0 µmols of Cobalt and various ratios of Manganese and Zinc were prepared. These solutions were evaporated dropwise in small aluminum pans heated to 130°C and reduced to salts. EDX was preformed to determine the atomic percent of Manganese and Zinc in each sample. The experiment was repeated for three batteries made from α-MnO_2, 0.2% silica coated MnO_2, and 10% silica coated MnO_2. After Charge/Discharge cycling (200 cycles), 1 mL of 0.022 M oxalic acid solution was added to each battery case and swirled around until deposited MnO_2 was dissolved. The liquids were removed to respective vials, and 200 µL of 4 mM Cobalt (II) acetate solution was added as the internal standard to each vial.

3. Results and Discussion

3.1 Material Characterization

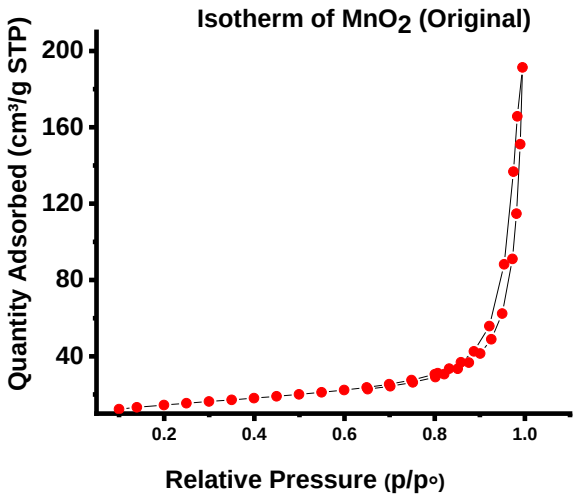

Silica Coating Amount (%wt.)	Surface Area (m^2/g)
OMS-2 (Parent material)	79.69
10% Silica	51.59
5% Silica	70.56
2% Silica	47.90
1% Silica	40.47
0.5% Silica	75.84
0.2% Silica	56.00
0.1% Silica	41.29
0.05% Silica	58.56

Figure 1. N_2-sorption Isotherm of α-MnO_2 material and BET surface area values of silica coated materials. Surface area remains consistent as silica content changes.

Cryptomelane-type α-MnO_2 nanorods were synthesized and characterized using N_2-sorption, XRD, XPS, SEM, EDX, and TEM. Figure 1 shows the N_2-sorption isotherm plot of the α-MnO_2 parent material and the measured BET surface area values of each silica-coated sample. For all samples measured, N_2-sorption isotherm demonstrated type V adsorption isotherm with no hysteresis, indicating very similar textural properties for all samples (not shown). The

shape of the isotherm plot indicates that the MnO_2 parent material is non-porous. No significant trends in the surface area were observed. The slight decrease in surface area as the silica content increases may be due to the silica filling small cracks and voids in the parent material. Clumping of the MnO_2 powder or silica gel may also be affecting surface area measurements.

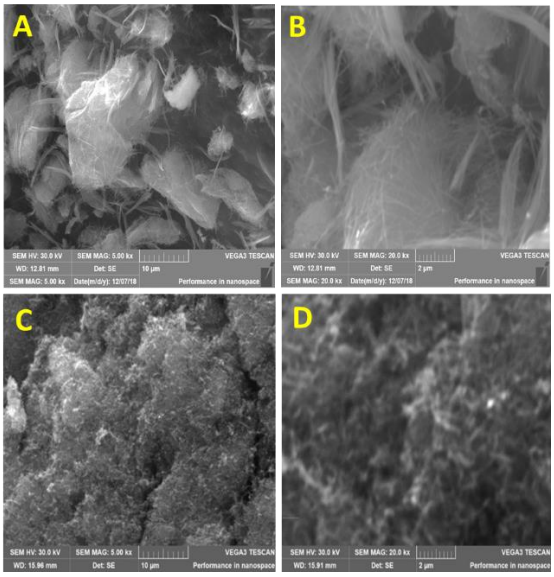

Figure 2. SEM images of A) α-MnO_2 at 5kx, B) α-MnO_2 at 20 kx, C) 0.2 % silica coating at 5kx, D) 0.2% silica at 20kx

Morphology studies of silica-coated MnO_2 using SEM (Figures 2A-2D) show that the structure of the nanorods is preserved throughout the silica-coating process and no separate SiO_2 agglomerates are observed. MnO_2 fibers are still visible after silica-coating, and the silica coating appears homogenous.

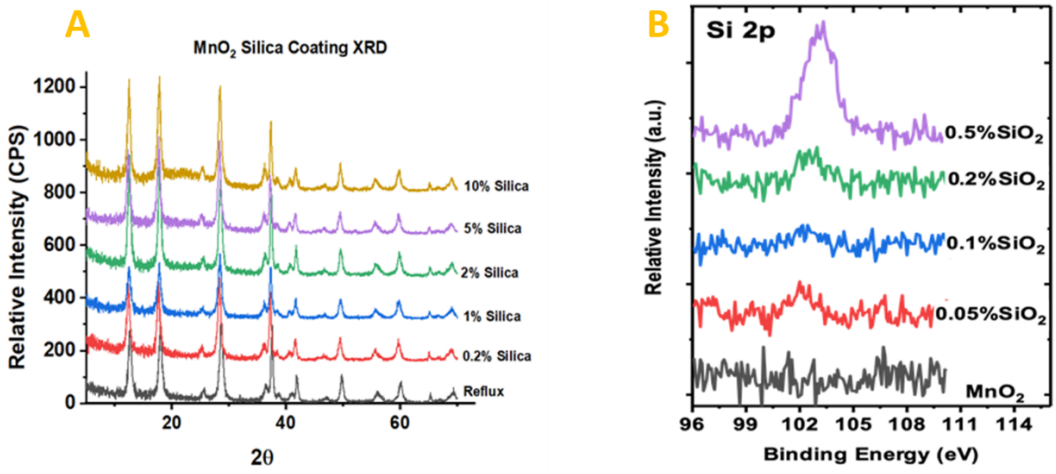

Figure 3. XRD and XPS of various SiO2 content MnO2.

Figure 3A shows the XRD patterns of various silica-content MnO_2 samples. Alignment of the peaks and similarity in peak intensity indicate that silica coating did not affect the crystal structure and crystallinity of the α-MnO_2 nanorods. The XPS spectra shown of low silica-content samples in Figure 3B also indicates that the synthesis procedure was successful in coating the nanorod surfaces in silica, as seen by the gradual intensification of the peak at 103 eV (Si_{2p}) as silica content increases. From XPS spectra, silica was detectible even at very low concentrations (0.05%) suggesting a surface coating.

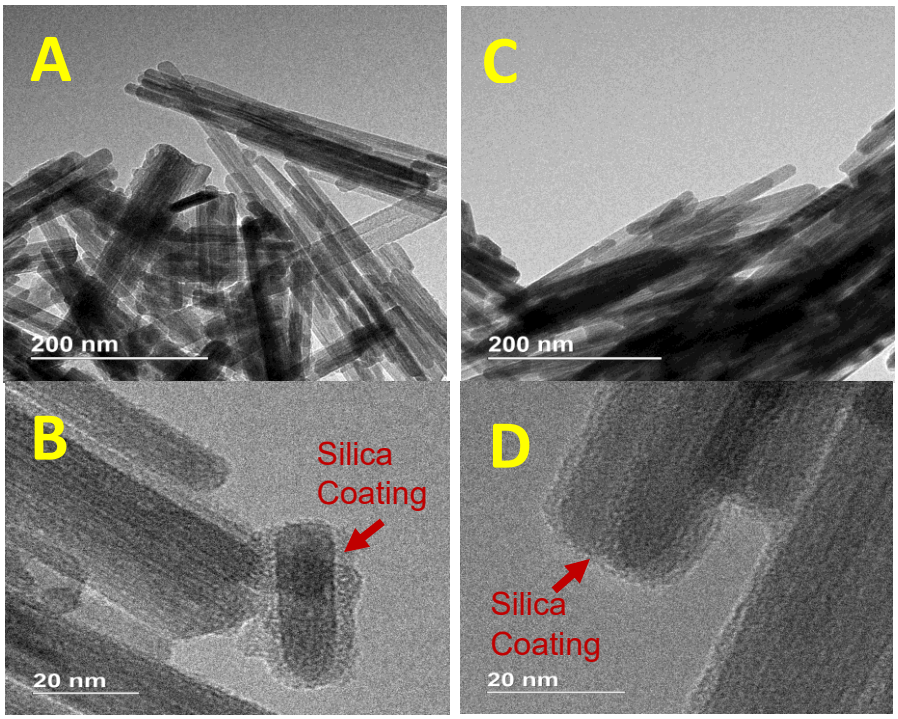

Figure 4. TEM images of A.) 2% silica at 200nm, B.) 2% silica at 20 nm C.) 0.1% silica at 200 nm D.) 0.1% silica at 20 nm.

In Figure 4, TEM images better show the preservation of the α-MnO_2 nanorods and the homogeneity of the silica coating. The silica layer on the 2% silica sample in Figure 4B is approximately 4-5 nm thick and coats the nanorod evenly with minor bumps and ridges. At a lower silica content of 0.1%, the coating thickness was substantially thinner, ~1-2 nm. Regardless of the silica coating amounts, the parent α-MnO_2 nanorods preserved their morphology and dimensions. α-MnO_2 nanorods are 20-30 nm in width and 200-400 nm in length. In summary, the sol-gel silica coating procedure reported here has no effect on the crystal structure, crystallinity, or morphology of the parent α-MnO_2 nanorods. The coating is homogenous throughout the samples studied.

3.2 Electrochemistry

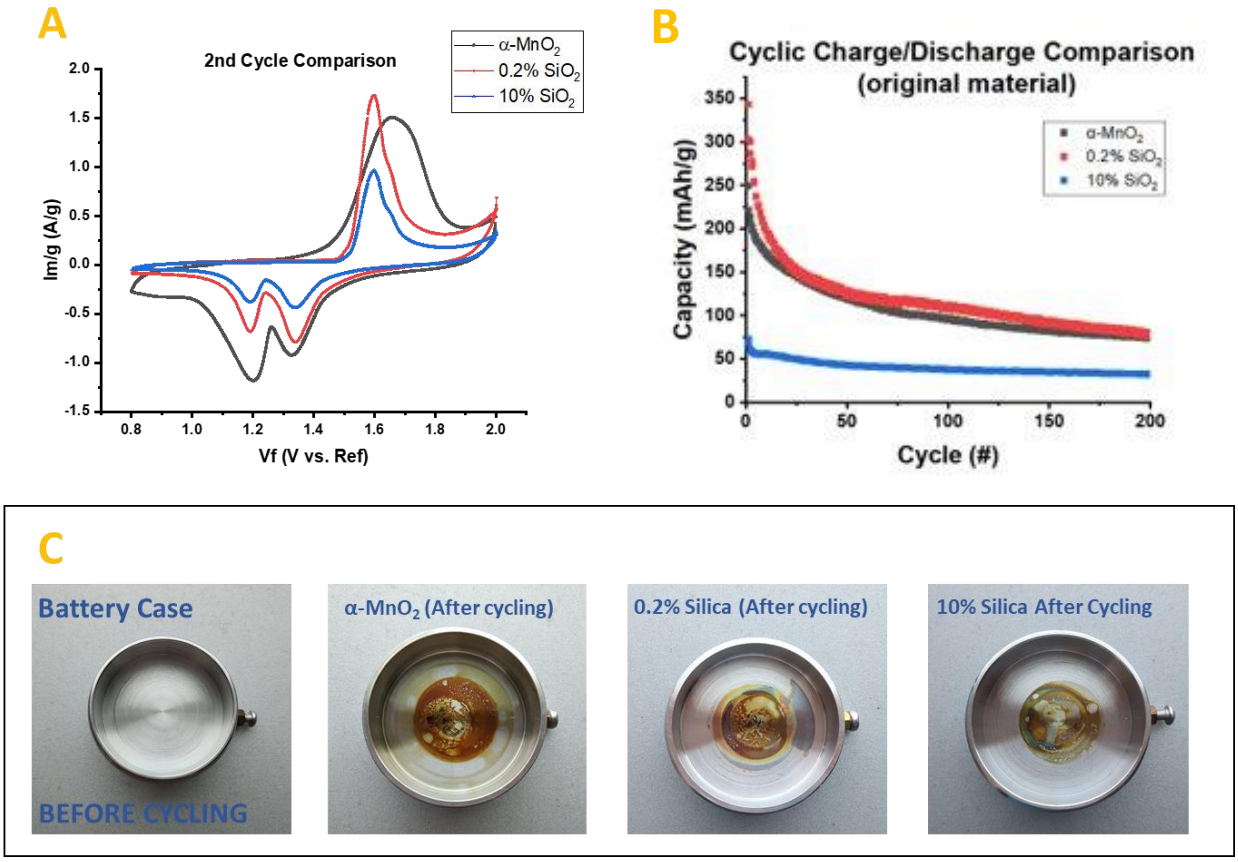

Figure 5. A) Cyclic Voltammetry performed between 0.8 V and 2.0 V at 0.5 mV/s for 4 cycles. B) Cyclic Charge/Discharge performance of α-MnO_2, 0.2% silica, and 10% silica. Cycling tests were performed between 0.9 V and 1.9 V at 500 mA/g rate. C) Images of the battery case before and after 200 Charge/Discharge cycles.

Batteries were assembled from electrodes made from α-MnO_2, 0.2% silica, and 10% silica-coated α-MnO_2. Cyclic Voltammetry (CV) and Cyclic Charge/Discharge (CD) tests were conducted. Figure 5A shows the overlaid CV plots of α-MnO_2 at the second cycle. The most notable difference between the CV plot of the battery made from the α-MnO_2 cathode material and those of the silica-coated materials is the shift in the anodic peak of α-MnO_2. The parent α-MnO_2 showed a broad oxidation (anodic) peak centered at 1.7 V. This peak is potentially two overlapping oxidation peaks, based on its broadness and shape. Upon silica coating, the oxidation peaks became narrower and the peak potentials were at 1.6 V for both of the silica coated samples. This could mean that one of the redox reactions is due to the cathode surface and the process is suppressed by silica coating. The CV plots for the batteries made from 0.2% silica and 10% silica-coated α-MnO_2 also exhibit a small shoulder, which also supports our assignment on surface reaction. Overall, the intensities of the oxidation and reduction peaks are significantly reduced by silica coating, suggesting that silica coating might impede zinc insertion during the discharge process. Figure 5B also shows the Charge/Discharge cycling performance of the three batteries over 200 cycles. Capacity is reported in mAh/g to account for the various amounts of MnO_2 cathode material present on each electrode. While 0.2% silica coating did not affect the cycling performance of the battery, 10% silica coating severely weakened the capacity. However, 10% silica-coated cathode material exhibits much greater capacity retention. After 50 cycles, the 10% silica battery's capacity retention was 57% compared the 0.2% silica battery, whose capacity after 50 cycles was only 38%. The capacity of the 0.2% silica battery starting at 350 mAh/g, higher than that of the α-MnO_2 could be due to error originating from a low amount of active material on the electrode.

Images of the battery cases before and after cycling are also shown in the Figure 5C. The brown color in the bottom of each battery case after cycling is due to the electrodeposition of the dissolved cathode material. Visually, even just 0.2% silica coating is extremely effective in preventing cathode dissolution. We further investigated the amount of dissolved cathode by quantifying the deposited manganese amounts on the battery case.

Sample (#)	Amount Mn (µmols)	Amount Zn (µmols)	Amount Co (µmols)
1	0.2	1.0	2.0
2	0.4	1.0	2.0
3	0.6	1.0	2.0
4	0.8	1.0	2.0
5	1.0	1.0	2.0
6	1.0	0.2	2.0
7	1.0	0.4	2.0
8	1.0	0.6	2.0
9	1.0	0.8	2.0
10	1.0	0	2.0

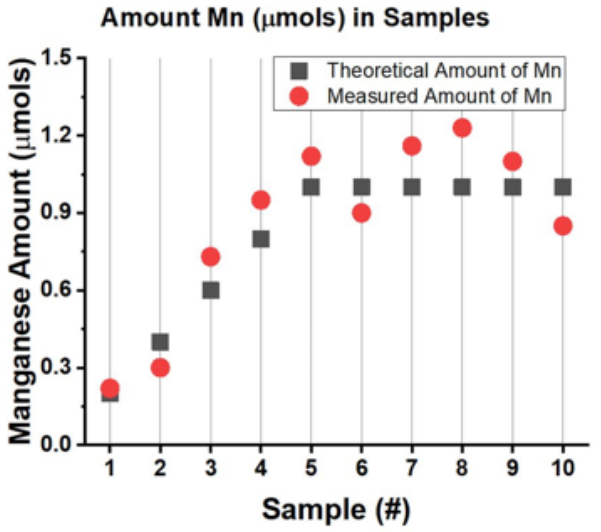

Silica Coating Amount (% wt.)	Among Active Material Dissolved (% wt.)
α-MnO_2	28%
0.2%	16%
10%	1.1%

Figure 6. 10-sample control experiment using various amounts of Manganese, Zinc, and Cobalt. Calibration plot and table of Manganese, Zinc, and Cobalt amounts. EDX quantification of these 10 samples using Cobalt as an internal standard and percent active material dissolved for three different cycled materials. Percent (wt.) dissolution was determined using EDX to analyze the atomic percent of Manganese deposited on the battery case after cycling and normalizing the atomic percent using a known internal standard Cobalt.

A dissolution experiment using EDX was conducted to quantify the cathode dissolution after 200 cycles at 500 mAh/g rate. A control experiment was first conducted. A table of the various ratios of Manganese to Zinc in each vial and the calibration plot after EDX was performed are shown above in Figure 6. The calibration plot shows that the developed EDX-based quantification methods can reliably detect the amounts of manganese (dissolved cathodes) on a sub-micromole level. The experiment was repeated to determine the percent weight of Manganese that was deposited into the bottom of each battery case after cycling. Without silica coating, 28% of the MnO_2 cathode material is dissolved and deposited into the battery case. It is noteworthy that this study does not report the amount of manganese in the electrolyte since most of the dissolved manganese is deposited on the battery case and its amounts will be much lower in the electrolyte. However, a 0.2% silica coating successfully reduced the amount of cathode material lost by nearly half, and 10% silica coating nearly eliminated dissolution.

3.4 Characterization of Used Electrodes

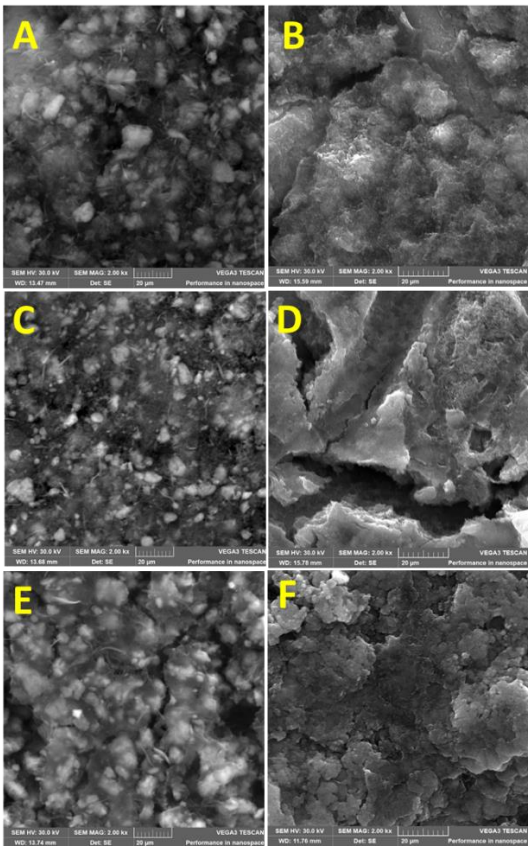

Figure 7. SEM images at 2.00 kx before and after Charge/Discharge cycling (200 cycles, 500 mA/g). A) α-MnO_2 (before), B) α-MnO_2 (after), C) 0.2% silica coating (before), D) 0.2% silica coating (after), E) 10% silica coating (before), F) 10% silica coating (after).

A morphology study of the used electrodes was carried out using SEM. Figure 7 shows significant surface degradation after 200 cycles. In all three samples, nanorods were no longer visible after cycling, and degradation of the electrodes is evident by the flaking on the surface (Figures 7B, 7D, 7F).

4. Conclusion

In summary, α-MnO_2 nanorods were successfully synthesized and SiO_2 surface coating greatly mitigated cathode dissolution. Physiochemical characterization of the α-MnO_2 (parent material) showed that it is non-porous. Characterization of silica-coated MnO_2 samples of various percent weights showed that silica coating did not affect the structure of the MnO_2 nanorods and that the surface coating is homogenous. Batteries were made from α-MnO_2, 0.2% silica, and 10% silica in order to study the effects of silica coating on battery performance and cathode dissolution. The dissolution experiment conducted showed that without silica coating, 28% of the active material is dissolved and deposited on the battery case. 0.2% silica coating reduced the percent weight of active material lost from 28% to 16% and only slightly reduced the battery performance over 200 cycles. 10% silica coating reduced the percent active material lost to just 1.1%. However, CV and Charge/Discharge data showed that Zinc insertion was inhibited and cycling performance suffered greatly. Further studies would investigate using a hydrothermal technique to synthesize sturdier nanorods. This would promote more even silica coating and hopefully prolong battery life by delaying cathode dissolution.

5. Acknowledgments

The authors would like to thank Creative Activities and Research Experiences for Team (CARET) Funding Award (2018-2019) and Kennesaw state University Department of Chemistry and Biochemistry for the continuous support and funding. M.H. and Z.Z. equally contributed to the manuscript.

6. References

1. Jiang, Baozheng, Chengjun Xu, Changle Wu, Liubing Dong, Jia Li, and Feiyu Kang. 2017. Manganese sesquioxide as cathode material for multivalent zinc ion battery with high capacity and long cycle life. *Electrochimica Acta* 229 (March 1,): 422-8. (accessed Jun 10, 2019).

2. Poyraz, Altug S., Josh Laughlin, and Zeljka Zec. 2019. Improving the cycle life of cryptomelane type manganese dioxides in aqueous rechargeable zinc ion batteries: The effect of electrolyte concentration. *Electrochimica Acta* 305 (May 10,): 423-32. (accessed Jun 6, 2019).

3. Wang, Fei, Oleg Borodin, Tao Gao, Xiulin Fan, Wei Sun, Fudong Han, Antonio Faraone, Joseph A. Dura, Kang Xu, and Chunsheng Wang. 2018. Highly reversible zinc metal anode for aqueous batteries. *Nature Materials* 17 (6) (-06): 543-9. (accessed Jun 10, 2019).

4. Cui, Jiajie, Xianwen Wu, Sinian Yang, Chuanchang Li, Fang Tang, Jian Chen, Ying Chen, Yanhong Xiang, Xianming Wu, and Zeqiang He. 2018. Cryptomelane-type KMn 8 O 16 as potential cathode material - for aqueous zinc ion battery. *Frontiers in Chemistry* 6 : 352. (accessed Jun 4, 2019).

5. Alfaruqi, Muhammad Hilmy, Saiful Islam, Dimas Yunianto Putro, Vinod Mathew, Sungjin Kim, Jeonggeun Jo, Seokhun Kim, Yang-Kook Sun, Kwangho Kim, and Jaekook Kim. 2018. Structural transformation and electrochemical study of layered MnO_2 in rechargeable aqueous zinc-ion battery. *Electrochimica Acta* 276 (June 20): 1-11. (accessed Jun 4, 2019).

6. Ling, Chen, and Ruigang Zhang. 2017. Manganese dioxide as rechargeable magnesium battery cathode. *Frontiers in Energy Research* 5. (accessed Jun 2, 2019).

7. Fang, Guozhao, Jiang Zhou, Anqiang Pan, and Shuquan Liang. 2018. Recent advances in aqueous zinc-ion batteries. *ACS Energy Letters* 3 (10) (October 12,): 2480-501.(accessed Jun 10, 2019).

8. Lee, Yoon Koo, Jonghyun Park, and Wei Lu. 2019. A comprehensive experimental and modeling study on dissolution in li-ion batteries. *Journal of the Electrochemical Society* 166 (8).(accessed Jun 6, 2019).

9. Li, C., H. P. Zhang, L. J. Fu, H. Liu, Y. P. Wu, E. Rahm, R. Holze, and H. Q. Wu. 2006. Cathode materials modified by surface coating for lithium ion batteries. *Electrochimica Acta* 51 (19) (May 20,): 3872-83. (accessed Jun 10, 2019).